HHS Public Access

Author manuscript

Sci Immunol. Author manuscript; available in PMC 2020 March 13.

Published in final edited form as:

Sci Immunol. 2019 September 13; 4(39): . doi:10.1126/sciimmunol.aaw7636.

Inhibition of IL-2 responsiveness by IL-6 is required for the generation of GC-T_{FH} cells.

Amber Papillion[1], **Michael D. Powell**[2,3], **Danielle A. Chisolm**[4], **Holly Bachus**[1], **Michael J. Fuller**[1], **Amy S. Weinmann**[4], **Alejandro Villarino**[5], **John J. O'Shea**[5], **Beatriz León**[4], **Kenneth J. Oestreich**[2,6,7], **André Ballesteros-Tato**[1,*]

[1]Department of Medicine, Division of Clinical Immunology and Rheumatology, University of Alabama at Birmingham, Birmingham, AL, USA.

[2]Virginia Tech Carilion Research Institute, Roanoke, VA, USA.

[3]Translational Biology, Medicine, and Health Graduate Program, Virginia Tech Carilion Research Institute, Roanoke, VA, USA.

[4]Department of Microbiology, University of Alabama at Birmingham, Birmingham, AL, USA.

[5]Molecular Immunology and Inflammation Branch, NIAMS, NIH, Bethesda, MD, USA.

[6]Virginia Tech Carilion School of Medicine, Roanoke, VA, USA.

[7]Department of Biomedical Sciences and Pathobiology, Virginia-Maryland College of Veterinary Medicine, Virginia Tech, Blacksburg, VA, USA.

Abstract

Sustained TCR stimulation is required for maintaining germinal center T follicular helper cells (GC-T_{FH}). Paradoxically, TCR activation induces interleukin-2 receptor (IL-2R) expression and IL-2 production, thereby initiating a feedback loop of IL-2 signaling that normally inhibits T_{FH} cells. It is unclear how GC-T_{FH} cells can receive prolonged TCR signaling without succumbing to the detrimental effects of IL-2. Using an influenza infection model, we show here that GC-T_{FH} cells secreted large amounts of IL-2 but responded poorly to it. Importantly, to maintain their IL-2-hyporesponsiveness, GC-T_{FH} cells required intrinsic interleukin-6 (IL-6) signaling. Mechanistically, we found that IL-6 inhibited upregulation of IL-2Rβ (CD122) by preventing

*__Corresponding author__ : andreballesterostato@uabmc.edu.

AUTHOR CONTRIBUTIONS.

A.P. performed the experiments with help from H.B., M.J.F. and A.B.-T. A.B.-T. and A.P. analyzed the data. A.B.-T. wrote the manuscript. A.B.-T. designed the experiments with the help of A.P and B.L. A.P, M.J.F and B.L. contributed to data interpretation and manuscript editing. A.B.-T., A.P., M.J.P., and K.J.O., did the statistical analysis. M.J.P. and K.J.O. performed the ChIP experiments. D.A.C. and A.S.W. performed the ATAC-seq analysis. A.V. and J.J.O. provided mice and expertise that were critical to this work. All authors reviewed the manuscript before submission.

COMPETING INTERESTS

The authors declare that they have no competing interests.

DATA AVAILABILITY.

The data that support the findings of this study are available from the corresponding author upon request. ATAC-seq data are available from GEO under accession code GSE124588. Non-commercially available mice and reagents generated in this study will be available upon request.

SUPPLEMENTARY MATERIALS

Supplementary material and methods

association of STAT5 with the *Il2rb* locus, thus allowing GC-T_{FH} cells to receive sustained TCR signaling and produce IL-2 without initiating a TCR/IL-2-inhibitory feedback loop. Collectively, our results identify a regulatory mechanism that controls the generation of GC-T_{FH} cells.

ONE SENTENCE SUMMARY

IL-6-mediated inhibition of CD122 allows T_{FH} cells to receive TCR signaling without initiating an inhibitory TCR/IL-2 loop.

INTRODUCTION

T follicular helper (T_{FH}) cells are a subset of $CD4^+$ T cells that provide survival and differentiation signals for the development and maintenance of the germinal centers (GCs) (1, 2). T_{FH} cells are primed outside of B cell follicles by antigen (Ag)-bearing dendritic cells (DCs) (3–6). This early stage of the T_{FH} cell response is independent of the presence of B cells (3, 4, 7) and is termed the “DC-phase.” Following their initial interaction with DCs, CXCR5 guides T_{FH} cells into the B/T cell border, where engagement of ICOS and PD-1 by bystander B cells directs T_{FH} cells into B cell follicles (3, 8, 9). Once inside the follicles, the interaction of GC-T_{FH} cells with activated B cells leads to the formation of GCs (1, 2), where persistent Ag presentation by GC B cells sustains the T_{FH} cell response (4, 5, 10, 11).

Interleukin-2 (IL-2) signaling inhibits T_{FH} cell differentiation by repressing Bcl-6 expression via STAT5 (12–14). Consequently, T_{FH} cell responses fail to develop in high-IL-2 environments (14–16). Strikingly, T_{FH} cells produce large amounts of IL-2 upon *in vitro* re-stimulation (17), and a recent study indicates that IL-2-producing cells are the precursors of T_{FH} cells (18). This is particularly intriguing since prolonged TCR stimulation, which is required for normal T_{FH} cell responses (5, 10), normally promotes IL-2R expression, thereby initiating a positive-feedback loop of IL-2/STAT5 signaling that results in increased IL-2 responsiveness (19, 20). Thus, the exact mechanisms that allow T_{FH} cells to receive sustained TCR stimulation without responding to IL-2 are unclear.

Whereas IL-2 inhibits Bcl-6 expression, IL-6 signaling via STAT3 transiently induces Bcl-6 up-regulation (21, 22). The role of IL-6 in T_{FH} cells is, however, puzzling. Although antiviral T_{FH} cell responses are normally initiated in the absence of IL-6/IL-6R interactions (23–25), intrinsic IL-6 signaling is critical for sustaining T_{FH} cell responses during the late stages of chronic viral infections (24). These data suggest that IL-6 signaling is not absolutely required for the initiation of the T_{FH} cell program but is essential for supporting antiviral T_{FH} responses during the GC-phase. The mechanisms by which IL-6 signaling contribute to the development of GC-T_{FH} cells are unknown.

Using an influenza infection model, we show here that IL-6 was dispensable for the initial priming of influenza-specific T_{FH} cells but was critical for the generation of GC-T_{FH} cells. Our results demonstrate that fully differentiated GC-T_{FH} cells produced large amounts of IL-2 and that intrinsic IL-6 signaling was required for maintaining their IL-2 hyporesponsiveness. Mechanistically, IL-6 negatively regulated CD122 expression, thus

preventing the initiation of a negative TCR/IL-2-feedback loop that inhibits the generation of GC-T_{FH} cells during the non-GC to GC-T_{FH} transition phase.

RESULTS

GC-T_{FH} cells require intrinsic IL-6 signaling

To study the role of IL-6 in the influenza-specific T_{FH} cell response, we infected C57BL/6 (WT) and C57BL/6.*Il6*$^{-/-}$ (*Il6*$^{-/-}$) mice with influenza and followed the kinetics of the nucleoprotein (NP)-specific T_{FH} cells in the lung-draining mediastinal lymph node (mLN) (Fig. 1A,B). The frequency (Fig. 1A) and number (Fig. 1B) of Bcl-6^{hi}CXCR5^{hi} NP-specific T_{FH} cells were similar in WT and *Il6*$^{-/-}$ mice early after infection (d7). However, the NP-specific T_{FH} cell response prematurely contracted in *Il6*$^{-/-}$ mice (Fig. 1A,B). Similar results were obtained in WT mice treated with anti-IL6 + anti-IL-6R (anti-IL6/R) blocking Abs (Fig. S1A).

To test whether IL-6 was required beyond the priming phase, we transferred CD45.1^{+} and CD45.1^{+}/2^{+} OTII cells into congenically different WT or *Il6*$^{-/-}$recipient mice (Fig. 1C). One day later, the recipient mice were infected with an engineered PR8 influenza virus expressing the OVA$_{323–339}$ peptide (PR8-OTII) (26). Three days after infection, CD4^{+} T cells from WT and *Il6*$^{-/-}$ recipients were purified and mixed so that the mixture contained equivalent numbers of CD45.1^{+} (WT-primed) and CD45.1^{+}/2^{+} (*Il6*$^{-/-}$-primed) OTII cells. As expected, OTII cells recovered from WT and *Il6*$^{-/-}$ primary recipient mice contained similar frequencies of Bcl-6^{hi}CXCR5^{hi} T_{FH} cells (Fig. S1B). Cell numbers were then normalized to the concentration of OTII cells and a 1:1 mixture of WT and *Il6*$^{-/-}$-primed OTII cells was transferred into day 5 infected WT or *Il6*$^{-/-}$secondary recipient mice. We found that regardless of whether OTII cells were initially primed in a WT or *Il6*$^{-/-}$ environment, nearly 30% of the donor OTII cells were T_{FH} cells in the WT mice on day 11 after infection (Fig. 1D,E and S1C). In contrast, less than 12% of the WT and *Il6*$^{-/-}$-primed OTII cells displayed a T_{FH} cell phenotype in the *Il6*$^{-/-}$ recipient mice (Fig. 1D,E and Fig. S1C). These results indicated that T_{FH} cell responses at the peak of the infection were compromised in the absence of IL-6, regardless of whether CD4^{+} T cells were primed in an IL-6-sufficient environment.

T follicular regulatory (Tfr) cells suppress T_{FH} cell responses in some models (27). The frequency and phenotype of Tfr cells was, however, similar in WT and IL-6$^{-/-}$ mice (Fig. S1D and E). Hence, changes in Tfr cells were not likely responsible for the diminished T_{FH} cell response observed in the *Il-6*$^{-/-}$ mice. We next assessed whether the requirement for IL-6 signaling was T cell-intrinsic. To do this, we infected WT/*Il6r*$^{-/-}$ mixed bone marrow (BM) chimeras (Fig. 1F) with influenza and determined the frequency of T_{FH} cells within the WT and *Il6r*$^{-/-}$ NP-specific CD4^{+} T cell compartments at different times after infection (Fig. 1G). The frequency of NP-specific T_{FH} cells was similar at day 7 (Fig. 1G). In contrast, NP-specific T_{FH} cells failed to accumulate in the *Il6r*$^{-/-}$ compared to WT compartment at day 10 after infection (Fig. 1G and H). These results indicated that IL-6 signaling beyond the initial priming phase was intrinsically required for the T_{FH} cell response to influenza. This conclusion was consistent with the presence of high levels of IL-6 during the post-priming phase of the primary response (Fig. S1F).

We next separated Bcl-6^{hi}CXCR5^{hi} NP-specific T_{FH} cells into PD-1^{hi} cells (GC-T_{FH}) and PD-1^{lo} cells (non-GC-T_{FH}) in our WT/*Il6r*$^{-/-}$ chimeras (Fig. 1I). The frequency of NP-specific Tfh cells with a non-GC-T_{FH} cell phenotype peaked at day 7 after infection and was similar in the WT and *Il6r*$^{-/-}$ donors at all time points analyzed (Fig. 1J). In contrast, the frequency of NP-specific Tfh cells with a GC-T_{FH} phenotype peaked between days 10 and 15 and was significantly diminished in the *Il6r*$^{-/-}$ relative to the WT compartment (Fig. 1K). As a result, the WT: *Il6r*$^{-/-}$ ratio of GC-T_{FH} was increased compared to the ratio of non-GC-T_{FH} or total CD4^{+} T cells (Fig. 1L). These results indicated that the diminished T_{FH} cell response observed in the absence of IL-6 signaling was due to the lack of influenza-specific GC-T_{FH} cells. In agreement with this, whereas the frequency of extrafollicular CD138^{+} antibody-secreting cells (ASCs) was similar in WT and *Il6*$^{-/-}$ mice (Fig. S1G), the GC B cell response was reduced in *Il6*$^{-/-}$ relative to WT mice at the peak of the infection (Fig. S1H and I). Furthermore, though the number of GC B cells was similar in WT and *Il6*$^{-/-}$ mice at later time points (Fig. S1I), we observed a significant reduction in the long-term influenza-specific IgG2b and IgG2c levels in *Il6*$^{-/-}$ mice compared to WT mice (Fig. SJ). Our data suggested that IL-6 was dispensable for the priming on non-GC-T_{FH} cells but was intrinsically required for the generation of GC-T_{FH} cells during the non-GC to GC-T_{FH} cell transition.

Late IL-6 prevents IL-2 responsiveness of GC-T_{FH} cells

Given that IL-2 inhibits T_{FH} cell responses (12–14) and that IL-6 antagonizes IL-2 signaling in some models (28, 29), we decided to investigate whether the late requirement for IL-6 signaling correlated with changes in IL-2 production. Using *Il21*-mCherry-*Il2*-emGFP dual-reporter mice (30), we found that the vast majority of IL-2 producing cells were CD4^{+} T cells (Fig. 2A). Although IL-2 producing CD4^{+} T cells were detected early after infection, the frequency (Fig. 2A) and number (Fig. 2B) of these cells peaked at day 12 post-infection. The same results were obtained when IL-2-producing NP-specific CD4^{+} T cells were enumerated (Fig. 2C), or when we assessed IL-2 production by intracellular staining (Fig. S2A). We also found that close to 80% of the GC-T_{FH} cells were GFP/IL-2^{+} at day 12 (Fig. 2D). As expected, GFP/IL-2^{+} T_{FH} cells were also mCherry/IL-21^{+} (Fig. 2E). The capacity of GC-T_{FH} cells to secrete IL-2 was further confirmed by intracellular staining (Fig. S2B). Similar results were obtained when we analyzed IL-2 production by NP-specific Tfh cells (Fig. 2F). Importantly, while IL-2^{+} GC-T_{FH} cells were already detectable at day 7, they largely accumulated during the peak of the response (day 12) (Fig. 2G and H). These results indicated that GC-T_{FH} cells produce large amounts of IL-2 during the peak of the infection.

We next decided to increase IL-2 availability early after infection, a time during which T_{FH} cells normally developed in the absence of IL-6. Importantly, treatment of WT mice with recombinant IL-2 (rIL-2) doses ≥ 15,000 units (U) prevented Tfh cell responses (Fig. 3A). In contrast, no differences were detected with doses under the 15,000U threshold, which we will refer to as suboptimal doses (Fig. 3A). Thus, we treated influenza-infected WT mice with a suboptimal dose of rIL-2 or PBS, administered either control or anti-IL6/R Ab, and evaluated the NP-specific T_{FH} cell response on day 7 (Fig. 3B,C). Whereas rIL-2 or anti-IL-6/R Abs alone did not significantly affect the NP-specific T_{FH} cell response, NP-specific T_{FH} cells failed to accumulate in mice that received rIL-2 in combination with anti-IL-6/R

Abs. Similar results were obtained in WT and *Il6*$^{-/-}$ mice (Fig. S3A). These results suggested that the lack of IL-6 signaling lowered the threshold of IL-2 required for suppressing T_{FH} cell responses, thereby rendering T_{FH} cells more responsive to IL-2.

$CD25^{+}FoxP3^{+}T_{reg}$ cells consume IL-2 early after infection (31–34), thereby lowering the IL-2 environment and helping T_{FH} cell differentiation (15). Thus, we considered the possibility that IL-6 was dispensable early after infection because IL-2 consumption by T_{reg} cells was sufficient for lowering the IL-2 availability below the necessary threshold for T_{FH} cell suppression. To test this hypothesis, we infected FoxP3-DTR mice with influenza, depleted T_{reg} cells to increase IL-2 availability (31–34), and assessed whether early T_{FH} cell responses developed in the absence of IL-6 signaling (Fig. 3D,E). In agreement with our previous studies (15), the frequency (Fig. 3D) and number (Fig. 3E) of NP-specific T_{FH} cells were significantly reduced in T_{reg}-depleted relative to control mice. Importantly, however, the NP-specific T_{FH} cell response was further reduced in T_{reg}-depleted mice that received anti-IL6/R Abs (Fig. 3D,E). These data suggest that, when developing in a high IL-2 environment, IL-6 was required for preventing IL-2 mediated suppression of the T_{FH} cell response.

To examine whether IL-6 signaling was intrinsically required to limit IL-2 responsiveness of T_{FH} cells, we infected WT/*Il6r*$^{-/-}$ chimeras with influenza, treated them daily with a suboptimal dose of rIL-2 or control PBS, and analyzed WT and *Il6r*$^{-/-}$ T_{FH} cells on day 7 after infection (Fig. 3F), a time during which WT and *Il6r*$^{-/-}$ T_{FH} cells similarly accumulated (Fig. 1G). As expected, the frequency of NP-specific T_{FH} cells within the WT and *Il6r*$^{-/-}$ compartments were comparable in the PBS-treated mice (Fig. 3F). In contrast, the frequency of *Il6r*$^{-/-}$ NP-specific T_{FH} cells was significantly diminished in the rIL-2 treated mice (Fig. 3F). These results indicated that intrinsic IL-6 signaling protected T_{FH} cells from IL-2-mediated suppression.

To confirm these conclusions, we carried out an *in vitro* study to test whether the presence of IL-6 affected the threshold of IL-2 required to prevent Bcl-6 expression. Carboxyfluorescein succinimidyl ester (CFSE)-labeled $CD4^{+}$ T cells were activated *in vitro* in the presence of increasing concentrations anti-IL-2 neutralizing Abs and either rIL-6 or control PBS. Bcl-6 expression in proliferating ($CFSE^{lo}$) $CD4^{+}$ T cells was measured two days later by flow cytometry (Fig. 3G). Proliferating $CD4^{+}$ T cells cultured in the absence of anti-IL-2 neutralizing Abs (i.e. high IL-2 conditions) expressed low levels of Bcl-6 (Fig. 3G). Bcl-6 expression, however, gradually increased with progressively higher concentrations of anti-IL-2 Abs (i.e. low IL-2 conditions) (Fig. 3G). Importantly, in the presence of IL-6, a lower concentration of anti-IL-2 Ab was required to promote Bcl-6 up-regulation (Fig. 3G). $CD4^{+}$ T cells proliferated at a similar rate in all conditions (Fig. S3B). These data suggested that intrinsic IL-6 signaling prevented IL-2 responsiveness of T_{FH} cells, which was required for sustaining T_{FH} cell responses when present in a high-IL-2 environment.

IL-6 prevents IL-2 responsiveness by inhibiting CD122 expression

TCR stimulation, which is required for the maintenance of the GC-T_{FH} cells (4, 5, 10, 11), induces CD25 expression. Given that IL-6 signaling negatively regulates CD25 expression (28, 35, 36), we considered the possibility that IL-6 signaling inhibited IL-2 responsiveness

of GC-T_{FH} cells by preventing CD25 upregulation. To test this idea, we infected WT and *Il6*$^{-/-}$ mice with influenza and assessed the expression of CD25 on NP-specific GC-T_{FH} cells and NP-specific T_{EFF} cells at different times after infection (Fig. 4A,B). *Il6*$^{-/-}$ NP-specific T_{EFF} cells expressed higher amounts of CD25 relative to WT controls early after infection (Fig. 4A). We found, however, that CD25 was virtually undetectable in both WT and *Il6*$^{-/-}$ NP-specific GC-T_{FH} cells (Fig. 4B). We next infected WT/*Cd25*$^{-/-}$ mixed BM chimeras, treated them with control or anti-IL-6/R Abs, and enumerated WT and *Cd25*$^{-/-}$ NP-specific GC-T_{FH} cells on day 10 after infection (Fig. 4C). The NP-specific $CD4^+$ T cells developed comparably from WT and *Cd25*$^{-/-}$ donors in both groups (Fig. S4A). As expected, WT GC-T_{FH} cells failed to accumulate in the anti-IL-6/R treated mice relative to control counterparts (Fig. 4C). However, treatment with anti-IL-6/R Abs also prevented the accumulation of *Cd25*$^{-/-}$ NP-specific GC-T_{FH} cells (Fig. 4C). These results suggested that IL-6 controlled the threshold of IL-2 responsiveness of T_{FH} cells by a CD25-independent mechanism

We next studied whether IL-6 deficiency resulted in changes in CD122 levels. We found that the expression of CD122 was increased in both *Il6*$^{-/-}$ NP-specific T_{EFF} (Fig. 4D) and NP-specific GC-T_{FH} cells (Fig. 4E and Fig. S4B) relative to WT counterparts. Similar results were obtained when we analyzed total GC-T_{FH} cells (Fig. S4C). To determine whether IL-6 signaling was intrinsically required for preventing CD122 up-regulation on GC-T_{FH} cells, we analyzed CD122 expression in WT and *Il6r*$^{-/-}$ NP-specific GC-T_{FH} cells from WT/*Il6r*$^{-/-}$ chimeras. We found that *Il6r*$^{-/-}$ NP-specific GC-T_{FH} cells were $CD122^{hi}$ compared to WT NP-specific GC-T_{FH} cells (Fig. 4F). To confirm the effect of IL-6 on CD122 expression, we analyzed CD25 (Fig. 4G) and CD122 (Fig. 4H) expression *in vitro*. As expected, $CFSE^{lo}$-$CD4^+$ T cells expressed high levels of CD25 in control conditions, but progressively downregulated CD25 in the presence of increasing concentrations of anti-IL-2 Ab (Fig. 4G). The presence of rIL-6 did not significantly change the dynamics of CD25 expression (Fig. 4G). However, whereas $CD25^{lo}$ cells generated under anti-IL-2 Ab conditions expressed high levels of CD122, $CD25^{lo}$ cells generated in the anti-IL-2 + rIL-6 conditions were $CD122^{lo}$ (Fig. 4H). Correlating with the differences in CD122 expression, $CD25^{lo}CD122^{lo}$ cells from the anti-IL-2 + rIL-6 cultures expressed higher levels of Bcl-6 compared to $CD25^{lo}CD122^{hi}$ cells generated in the presence of anti-IL-2 Ab alone (Fig. 4I). These data indicated that intrinsic IL-6 signaling negatively regulates CD122 expression; thereby preventing CD122 up-regulation on T_{FH} cells.

IL-21 and IL-6 overlap in their capacity to promote T_{FH} cell development (23). Thus, we used our *in vitro* system to test the capacity of IL-21 to regulate Bcl-6 (Fig. 4J), CD122 (Fig. 1K), and CD25 (Fig. 1L) expression. Similar to the anti-IL-2+rIL-6 conditions, cells cultured in the presence of anti-IL-2+rIL-21 up-regulated Bcl-6 (Fig. 4J) and downregulated CD122 (Fig. 4K) compared to cells activated in the presence of anti-IL-2 Abs alone. No differences were detected in CD25 (Fig. 4L). Next, we studied the T_{FH} cell response in WT and *Il21r*$^{-/-}$ mice infected with influenza (Fig. 4M–P). The frequency (Fig. 4M) and number (Fig. 4N) of NP-specific T_{FH} cells, and the frequency of NP-specific T_{FH} cells with a PD-1^{hi}-GC-T_{FH} cell phenotype (Fig. 4O) were similar in WT and *Il21r*$^{-/-}$ mice at all time points analyzed. We also found that WT and *Il21r*$^{-/-}$ NP-specific GC-T_{FH} cells expressed equivalent levels of CD122 (Fig. 4P). As a control, CD122 expression in NP-specific T_{FH}

cells was increased in WT and *Il21r*$^{-/-}$ mice treated with anti-IL-6/R Abs (Fig. S4D). These data indicated that, whereas IL-21 could replace IL-6 signaling *in vitro*, it was dispensable for down-regulating CD122 and promoting influenza-specific GC-T_{FH} responses *in vivo*. In contrast, IL-6 signaling was necessary and sufficient.

In the absence of IL-6, STAT5 deficiency rescues GC-T_{FH} cells

Given that IL-2-producing GC-T_{FH} cells largely accumulated at the peak of the response and that GC-T_{FH} cells express high levels of CD122, we hypothesized that the lack of GC-T_{FH} cells observed in the *Il6*$^{-/-}$ mice was due to excessive IL-2/STAT5 signaling. To determine whether increased CD122 expression in *Il6*$^{-/-}$ T_{FH} cells resulted in augmented responsiveness to IL-2, we stimulated cells from influenza-infected WT and *Il6*$^{-/-}$ mice with different concentrations of IL-2 and evaluated STAT5 phosphorylation in GC-T_{FH} cells (Fig. 5A and B). We found that pSTAT5 was increased in *Il6*$^{-/-}$compared to WT GC-T_{FH} cells (Fig. 5A and B). Next, we generated WT/*Stat5ab*$^{-/-}$ mixed BM chimeras (Fig. 5C), infected them with influenza, treated them or not with anti-IL-6/R Abs, and enumerated WT and *Stat5ab*$^{-/-}$ GC-T_{FH} cells on day 10 after infection (Fig. 5D and E). The frequency of WT GC-T_{FH} cells was reduced by about 50% in the anti-IL-6/R relative to control-treated mice (Fig. 5D). In contrast, the frequency of *Stat5ab*$^{-/-}$ GC-T_{FH} cells was similar in both groups (Fig. 5D). Similar results were obtained when we analyzed the NP-specific GC-T_{FH} cell response (Fig. 5E). These results suggested that IL-6 signaling during the non-GC to GC-T_{FH} cell transition phase prevented CD122 up-regulation, thereby limiting IL-2/Stat5 responsiveness and protecting GC-T_{FH} cells from the deleterious effect of IL-2.

IL-6 prevents association of STAT5 to the *Il2rb* locus

To better define the mechanisms by which IL-6 controls CD122 expression, we examined whether changes in CD122 expression in the absence of IL-6 correlated with changes in chromatin accessibility in the *Il2rb* locus in T_{FH} and T_{EFF} cells (Fig. 6A). We adoptively transferred naïve OTII (CD45.1^{+}) cells into WT or *Il6*$^{-/-}$ recipient mice that were then infected with PR8-OTII one day later. Seven days after infection, donor-derived T_{FH} and T_{EFF} cells were sorted from WT or *Il6*$^{-/-}$ recipients and chromatin accessibility was examined via transposase-accessible chromatin-sequencing (ATAC-seq). We observed differences in chromatin accessibility near the 5' end of the *Il2rb* locus between OTII-T_{FH} and OTII-T_{EFF} cells from WT recipients (Fig. 6A). Interestingly, the profile of the ATAC-seq peaks from OTII-T_{FH} cells from *Il6*$^{-/-}$ recipient mice resembled the profile obtained in OTII-T_{EFF} cells (Fig. 6A). As a control, no differences were detected in the *Il2ra* locus (Fig. S5A). These results indicated the presence of regulatory elements at the *Il2rb* locus that were responsive to IL-6 in T_{FH} and T_{EFF} cells.

CD122 expression is positively regulated in response to IL-2/STAT5 signaling (19, 20). Corresponding with this idea, using our WT/*Stat5ab*$^{-/-}$ chimeras we found that increased CD122 expression observed after IL-6 blockade was STAT5 dependent (Fig. 6B). Given that STAT3 competes with STAT5 for DNA binding to some of its target genes (29), we considered the possibility that IL-6 signaling prevented CD122 expression by interfering with the ability of STAT5 to associate to the *Il2rb* locus. Chromatin immunoprecipitation sequencing studies (ChIP-seq) have been performed previously to study binding of STAT3

and STAT5 to the *Il17a* locus (29). We reanalyzed these data and identified three STAT5 binding sites, one located at the promoter region (Region A), and two down-stream of the transcription start site (Regions B and C). STAT3 ChIP-seq peaks were found at the same sites, thus suggesting that STAT3 and STAT5 bound to the same regions of the *Il2rb* locus (Fig. S5). Next, we activated $CD4^+$ T cells in the presence of rIL-6 or control PBS and used ChIP-qRT-PCR to study whether IL-6 signaling affected STAT5 binding to the *Il2rb* locus (Fig. 6C–E). As expected, we observed reduced *Il2rb* expression in the IL-6 treated cells (Fig. 6C). We also found that STAT5 association to Regions A and B of the *Il2rb* locus was significantly diminished in the presence of IL-6 (Fig. 6D), which correlated with reduced gene expression (Fig. 6C). In contrast, STAT3 association at Region B was significantly enriched in IL-6 relative to control-stimulated cells (Fig. 6E). Collectively, our results indicated that IL-6/STAT3 signaling prevented association of STAT5 with the *Il2rb* locus, thereby preventing CD122 up-regulation and the subsequent initiation of a deleterious-feedback loop of TCR/IL-2/STAT5 signaling that results in increased responsiveness to IL-2.

DISCUSSION

Here we show that fully differentiated T_{FH} cells secrete large amounts of IL-2, a potent inhibitor of T_{FH} cells (12–14). Despite producing IL-2, however, T_{FH} cells were resistant to IL-2 signaling. Our data demonstrated that maintaining IL-2 hyporesponsiveness in T_{FH} cells during the non-GC to GC-T_{FH} cell transition was fundamental for the generation of influenza-specific GC-T_{FH} cells. Importantly, IL-6 did not limit IL-2 responsiveness by a CD25-dependent mechanism, but instead prevented CD122 expression. Mechanistically, IL-6 signaling inhibited CD122 up-regulation in response to TCR stimulation by preventing STAT5 association to the *Il2rb* locus, which precluded the initiation of a positive-feedback loop of TCR/IL-2/STAT5 signaling that would result in increased responsiveness to IL-2. Collectively, our results demonstrate that IL-6 signaling fine-tunes the threshold of IL-2 responsiveness of T_{FH} cells, allowing them to receive TCR stimulation and produce IL-2 without succumbing to its deleterious effects.

Our data suggest a model by which the requirement for IL-6 depends on the relative availability of IL-2, hence clarifying previous conflicting studies regarding the role of IL-6 in controlling T_{FH} cell responses. In this model, in the absence of IL-2, or when the environmental levels of IL-2 are below the minimum necessary threshold for T_{FH} cell suppression, IL-6 signaling is dispensable. In contrast, when the IL-2 availability exceeds the threshold for T_{FH} cell suppression, intrinsic IL-6 signaling is required for preventing IL-2 mediated suppression of the T_{FH} cell response. The environmental availability of IL-2 is the result of a tightly regulated balance between IL-2-producing and IL-2-consuming cells (15, 16, 31). This balance, however, varies throughout the infection depending on timing and anatomical location. For example, early after infection $CD25^+T_{reg}$ cells (15, 31) and $CD25^+$DCs (16) consume T cell-derived IL-2, thereby limiting IL-2 availability and favoring T_{FH} cell development during the DC phase. As the immune response to progresses, however, T_{FH} cells migrate into the B cell follicles where CD25-expressing cells are scarce. As such, T_{regs} in B cell follicles characteristically express low levels of CD25 (34, 37, 38) and $CD25^+$DCs preferentially localize outside the B cell follicles and quickly deregulate CD25 after activation (16). Thus, high density of IL-2-producing T_{FH} cells combined with the

scarcity of “IL-2 consumers” generates a relatively high-IL-2 environment during the non-GC to GC-T_{FH} transition phase. Under such conditions, IL-6 is required for preventing excessive IL-2 signaling and generating GC-T_{FH} cells.

The capacity of T_{FH} cells to produce IL-2 is not entirely surprising since sustained TCR stimulation, which is required for the maintenance of GC-T_{FH} cells, potently induces IL-2 production (4, 5, 10, 11, 39). Moreover, while Blimp-1 represses *Il2* transcription as part of a negative feedback loop that hinders IL-2 production after T cell activation (40, 41), Bcl-6 positively regulates IL-2 secretion (18). Thus, given that T_{FH} cells characteristically express high levels of Bcl-6, low levels of Blimp-1, and establish prolonged cognate interactions with APCs, it is likely that they will produce large amounts of IL-2. One caveat to our study is that, due to the lack of Tfh-conditional knock out mice, we did not examine the effect of IL-2 produced by Tfh cells. Thus, further investigations will be required to define the role played by IL-2-secreting T_{FH} cells in GC dynamics. In summary, our study indicates that T_{FH} cell homeostasis is controlled by a tightly regulated balance between the relative levels of IL-2 and IL-6, rather than by the absolute expression of IL-2 or IL-6 alone, thus offering a new perspective for how T_{FH} cell responses are regulated.

STUDY DESIGN

The goal of this study was to determine the role of IL-6 signaling in the T_{FH} cell response to influenza. Flow cytometry was used to characterize T_{FH} cells in WT and *Il-6*$^{-/-}$ mice at different times after infection. The main conclusions were validated using mixed bone marrow chimeras and molecular studies. All mice were infected with subtlethal doses of influenza virus. Mice did not receive supportive care, but body condition was monitored daily. A sample size of 4–5 mice/group/time-point was used for the *in vivo* experiments. This number was sufficient to generate enough cells for analysis and to detect statistically significant differences between groups while minimizing the use of laboratory animals. The investigators were not blinded when performing the experiments. Control and experimental groups were age and sex-matched. Males and females were used in these experiments.

MATERIALS AND METHODS

Mice.

C57BL/6 (B6), B6.SJL-*Ptprc*^{a} *Pepc*^{b}/BoyJ (B6.CD45.1), B6.129S2-IL6^{tm1Kopf}/J (*Il-6*$^{-/-}$), B6.129P2-*Tcrβ*^{tm1Mom} *Tcrδ*^{tm1Mom} (*Tcrb*$^{-/-}$ *Tcrd*$^{-/-}$), B6.129S4-*Il2ra*tm1Dw/J (*Cd25*$^{-/-}$), B6.Cg-Tg(Lck-cre)3779Nik/J, B6;SJL-Il6ra$^{tm1.1Drew}$/J (*Il6ra*$^{fl/fl}$), C57BL/6-Tg(TcraTcrb)425Cbn/J (OTII), B6.129S6-*Foxp3*tm1DTR (FoxP3-DTR), and B6N.129-Il21rtm1Kopf/J mice were originally obtained from Jackson Laboratories. *Il21*-mCherry-*Il2*-emGFP dual-reporter transgenic mice were obtained from W. J. Leonard (NHLBI). *Il6ra* $^{fl/fl}$ mice were crossed to B6.Cg-Tg(Lck-cre)3779Nik/J mice to generate B6. *Il6ra* $^{fl/fl}$ *1*$^{fl/fl}$-*Lck*$^{cre/+}$mice (*Il6r*$^{-/-}$). BM from *Stat5a/b*$^{fl/fl}$-*Cd4*$^{cre/+}$ mice was obtained from Dr. John J. O’Shea (National Institutes of Health) All mice were bred in the University of Alabama at Birmingham (UAB) animal facility. All experimental procedures involving animals were approved by the UAB Institutional Animal Care and Use Committee and were performed according to guidelines outlined by the National Research Council.

Infections, BM chimeras and *in vivo* treatments.

Infections were performed intranasally (i.n) with 6,500 VFU of A/PR8/34 (PR8) influenza virus in 100 μl of PBS or with 500 VFU of PR8-OTII influenza virus in 100 μl of PBS. BM chimeras were generated by irradiating the indicated recipient mice with 950 Rads from an X-ray source delivered in two equal doses administered 4–5 hours apart. Following the second dose of irradiation, mice were intravenously injected with 5 × 106 total BM cells and were allowed to reconstitute for 8–10 weeks before influenza infection. In indicated experiments, experimental animals received an intraperitoneal injection of 50 μg/kg of DT (Sigma) at the indicated time points. In some experiments, mice were intraperitoneally administered recombinant IL-2 (National Cancer Institute) at the indicated time points and doses. In some experiments mice were treated with 250 μg of a mix of anti-IL-6/R (15A7) and anti-IL-6 (MP5–20F3) neutralizing antibodies, both obtained from BioXcell.

Cell purification and adoptive transfer.

$CD45.1^+CD45.2^-$ and $CD45.1^+CD45.2^+$ OTII cells were purified from the spleens of naïve $CD45.1^+CD45.2^-$ and $CD45.1^+CD45.2^+$ OTII mice by positive selection with anti-CD4 beads (Miltenyi Biotec). Purified OTII cells (1×10^6) were transferred i.v into either B6 or *Il6*$^{-/-}$ recipient mice. One day later, the recipient mice were infected with PR8-OTII influenza virus. Three days after infection, $CD4^+$ T cells from the mLN of WT and *Il6*$^{-/-}$ recipient mice were positively selected with anti-CD4 beads (Miltenyi Biotec). Purified $CD4^+$ T cells were mixed so that the mixture contained a 1:1 ratio of $CD45.1^+CD45.2^-$ (WT-primed) and $CD45.1^+CD45.2^+$ (*Il6*$^{-/-}$-primed) OTII cells. Cell numbers were then normalized to the concentration of OTII cells and 2×10^3 cells of the 1:1 mixture of WT-primed and *Il6*$^{-/-}$-primed OTII cells were adoptively transferred into WT and *Il6*$^{-/-}$ mice that were previously infected with PR8-OTII influenza virus 5 days earlier.

In vitro studies.

Naïve CD4+ cells were purified from spleens of B6 mice using positive selection with anti-CD4 MACS beads (Miltenyi Biotec). Purified cells were activated with anti-CD3 (clone 145–2C11, 2.5μg/mL) and anti-CD28 (clone 37.51, 2.5μg/mL) antibodies in the presence of the indicated concentration of anti-IL-2 neutralizing antibodies (JES6–1A12 and S4B6–1, BioXcell) with or without rIL6 (R&D) at indicated concentrations. Cells were cultured for 48 h at 37 °C in 125 μl in round- bottomed 96-well plates in RPMI-1640 supplemented with sodium pyruvate, HEPES (pH 7.2–7.6 range), nonessential amino acids, penicillin, streptomycin, 2-mercaptoethanol and 10% heat-inactivated FCS (all from Gibco).

ATAC-seq analysis.

OTII ($CD45.1^+$) cells were adoptively transferred into WT (C57Bl/6) and *Il6*$^{-/-}$ recipient mice. One day later, recipient mice were infected with PR8-OTII. Seven days after infection, 30,000 donor-derived $CD45.1^+CXCR5^{hi}SLAM^{lo}CD4^+CD19^-$ T_{FH} and $CD45.1^+CXCR5^{lo}SLAM^{hi}$ $CD4^+CD19^-$ T_{EFF} cells were sorted from the mLN of WT and *Il6*$^{-/-}$ recipient mice using a FACSAria (BD Biosciences) and ATAC-seq was performed as previously described (42). Sorted T_{FH} and T_{EFF} cells were lysed in ice-cold lysis buffer (10mM TrisCl pH 7.4, 10mM NaCl, 3mM $MgCl_2$, 0.1% Igepal). Transposase reactions were

performed using Tn5 transposase (Illumina) and were incubated for 30 minutes at 37°C. DNA MinElut Kit (Qiagen) was used for DNA purification. Libraries were amplified using Nextara primers with NEBNext High-Fidelity 2X PCR Master Mix (New England Biolegends), and reactions were purified with the PCR Purification Kit (Qiagen). Libraries were sequenced on a 1×50 bp paired end run on a HiSeq2500 instrument in a rapid run mode at the University of Alabama at Birmingham Heflin Center for Genomic Science.

The raw fastq data files were trimmed to remove primer adapters using Trim Galore! version 0.4.1. Trimmed sequences were aligned to mm9 reference genome from UCSC using Bowtie2 version 2.2.9 with the option '-X. Aligned reads were then sorted followed by removal of duplicates using Picard version 2.6.0 SortSam and MarkDuplicates, respectively (Picard: http://broadinstitute.github.io/picard). Peak calling was then performed using Model-based Analysis of ChIP-seq (MACS2) callpeak version 2.1.1.20160309 using these options: '-B', '-q 0.05', '--call-summits', '—nomodel', '--nolambda', and --keep-dup all'. For visualization of the peaks in the UCSC Genome Browser (http://genome.ucsc.edu/), alignment files were normalized using deepTools version 2.3.3 bamCoverage using the options: '--normalizeTo1× 2150570000', and '--ignore For Normalization chrX chrM'.

Statistical analysis.

GraphPad Prism software (Version 7) was used for data analysis. The statistical significance of differences in mean values was determined using a two-tailed Student's *t* test. *P* values of less than 0.05 were considered statistically significant.

Supplementary Material

Refer to Web version on PubMed Central for supplementary material.

ACKNOWLEDGEMENTS.

The authors would like to thank W. J. Leonard (US National Institutes of Health) for providing the *Il21*-mCherry-*Il2*-emGFP dual reporter transgenic mice and T.S. Simpler, R. Burnham and U. Mudunuru for animal husbandry.

FUNDING.

This work was supported by the University of Alabama at Birmingham (UAB) and National Institutes of Health grants 1R01 AI110480 to A.B.-T, R01 AI116584 to B.L, R01AI061061 to A.W, R56AI127800 and R01AI134972 to K.J.O, and NIAMS Intramural Research Program funds to J.J.O. The X-RAD 320 unit was purchased using a Research Facility Improvement Grant, 1 G20RR022807–01, from the National Center for Research Resources, National Institutes of Health. Support for the UAB flow cytometry core was provided by grants P30 AR048311 and P30 AI027767.

REFERENCES

1. Qi H, T follicular helper cells in space-time. Nature reviews. Immunology 16, 612–625 (2016).
2. Vinuesa CG, Linterman MA, Yu D, MacLennan IC, Follicular Helper T Cells. Annual review of immunology 34, 335–368 (2016).
3. Choi YS, Kageyama R, Eto D, Escobar TC, Johnston RJ, Monticelli L, Lao C, Crotty S, ICOS receptor instructs T follicular helper cell versus effector cell differentiation via induction of the transcriptional repressor Bcl6. Immunity 34, 932–946 (2011). [PubMed: 21636296]

4. Goenka R, Barnett LG, Silver JS, O'Neill PJ, Hunter CA, Cancro MP, Laufer TM, Cutting edge: dendritic cell-restricted antigen presentation initiates the follicular helper T cell program but cannot complete ultimate effector differentiation. J Immunol 187, 1091–1095 (2011). [PubMed: 21715693]
5. Deenick EK, Chan A, Ma CS, Gatto D, Schwartzberg PL, Brink R, Tangye SG, Follicular helper T cell differentiation requires continuous antigen presentation that is independent of unique B cell signaling. Immunity 33, 241–253 (2010). [PubMed: 20691615]
6. Ballesteros-Tato A, Randall TD, Priming of T follicular helper cells by dendritic cells. Immunology and cell biology 92, 22–27 (2014). [PubMed: 24145854]
7. Baumjohann D, Okada T, Ansel KM, Cutting Edge: Distinct waves of BCL6 expression during T follicular helper cell development. J Immunol 187, 2089–2092 (2011). [PubMed: 21804014]
8. Xu H, Li X, Liu D, Li J, Zhang X, Chen X, Hou S, Peng L, Xu C, Liu W, Zhang L, Qi H, Follicular T-helper cell recruitment governed by bystander B cells and ICOS-driven motility. Nature 496, 523–527 (2013). [PubMed: 23619696]
9. Shi J, Hou S, Fang Q, Liu X, Liu X, Qi H, PD-1 Controls Follicular T Helper Cell Positioning and Function. Immunity 49, 264–274 e264 (2018). [PubMed: 30076099]
10. Baumjohann D, Preite S, Reboldi A, Ronchi F, Ansel KM, Lanzavecchia A, Sallusto F, Persistent antigen and germinal center B cells sustain T follicular helper cell responses and phenotype. Immunity 38, 596–605 (2013). [PubMed: 23499493]
11. Kerfoot SM, Yaari G, Patel JR, Johnson KL, Gonzalez DG, Kleinstein SH, Haberman AM, Germinal center B cell and T follicular helper cell development initiates in the interfollicular zone. Immunity 34, 947–960 (2011). [PubMed: 21636295]
12. Nurieva RI, Podd A, Chen Y, Alekseev AM, Yu M, Qi X, Huang H, Wen R, Wang J, Li HS, Watowich SS, Qi H, Dong C, Wang D, STAT5 protein negatively regulates T follicular helper (Tfh) cell generation and function. The Journal of biological chemistry 287, 11234–11239 (2012). [PubMed: 22318729]
13. Johnston RJ, Choi YS, Diamond JA, Yang JA, Crotty S, STAT5 is a potent negative regulator of TFH cell differentiation. The Journal of experimental medicine 209, 243–250 (2012). [PubMed: 22271576]
14. Ballesteros-Tato A, Leon B, Graf BA, Moquin A, Adams PS, Lund FE, Randall TD, Interleukin-2 inhibits germinal center formation by limiting T follicular helper cell differentiation. Immunity 36, 847–856 (2012). [PubMed: 22464171]
15. Leon B, Bradley JE, Lund FE, Randall TD, Ballesteros-Tato A, FoxP3+ regulatory T cells promote influenza-specific Tfh responses by controlling IL-2 availability. Nature communications 5, 3495 (2014).
16. Li J, Lu E, Yi T, Cyster JG, EBI2 augments Tfh cell fate by promoting interaction with IL-2-quenching dendritic cells. Nature 533, 110–114 (2016). [PubMed: 27147029]
17. Yu D, Rao S, Tsai LM, Lee SK, He Y, Sutcliffe EL, Srivastava M, Linterman M, Zheng L, Simpson N, Ellyard JI, Parish IA, Ma CS, Li QJ, Parish CR, Mackay CR, Vinuesa CG, The transcriptional repressor Bcl-6 directs T follicular helper cell lineage commitment. Immunity 31, 457–468 (2009). [PubMed: 19631565]
18. DiToro D, Winstead CJ, Pham D, Witte S, Andargachew R, Singer JR, Wilson CG, Zindl CL, Luther RJ, Silberger DJ, Weaver BT, Kolawole EM, Martinez RJ, Turner H, Hatton RD, Moon JJ, Way SS, Evavold BD, Weaver CT, Differential IL-2 expression defines developmental fates of follicular versus nonfollicular helper T cells. Science 361, (2018).
19. Malek TR, The biology of interleukin-2. Annual review of immunology 26, 453–479 (2008).
20. Au-Yeung BB, Smith GA, Mueller JL, Heyn CS, Jaszczak RG, Weiss A, Zikherman J, IL-2 Modulates the TCR Signaling Threshold for CD8 but Not CD4 T Cell Proliferation on a Single-Cell Level. J Immunol 198, 2445–2456 (2017). [PubMed: 28159902]
21. Liu X, Yan X, Zhong B, Nurieva RI, Wang A, Wang X, Martin-Orozco N, Wang Y, Chang SH, Esplugues E, Flavell RA, Tian Q, Dong C, Bcl6 expression specifies the T follicular helper cell program in vivo. The Journal of experimental medicine 209, 1841–1852, S1841–1824 (2012). [PubMed: 22987803]
22. Nurieva RI, Chung Y, Hwang D, Yang XO, Kang HS, Ma L, Wang YH, Watowich SS, Jetten AM, Tian Q, Dong C, Generation of T follicular helper cells is mediated by interleukin-21 but

independent of T helper 1, 2, or 17 cell lineages. Immunity 29, 138–149 (2008). [PubMed: 18599325]

23. Eto D, Lao C, DiToro D, Barnett B, Escobar TC, Kageyama R, Yusuf I, Crotty S, IL-21 and IL-6 are critical for different aspects of B cell immunity and redundantly induce optimal follicular helper CD4 T cell (Tfh) differentiation. PloS one 6, e17739 (2011).
24. Harker JA, Lewis GM, Mack L, Zuniga EI, Late interleukin-6 escalates T follicular helper cell responses and controls a chronic viral infection. Science 334, 825–829 (2011). [PubMed: 21960530]
25. Poholek AC, Hansen K, Hernandez SG, Eto D, Chandele A, Weinstein JS, Dong X, Odegard JM, Kaech SM, Dent AL, Crotty S, Craft J, In vivo regulation of Bcl6 and T follicular helper cell development. J Immunol 185, 313–326 (2010). [PubMed: 20519643]
26. Thomas PG, Brown SA, Yue W, So J, Webby RJ, Doherty PC, An unexpected antibody response to an engineered influenza virus modifies CD8+ T cell responses. Proceedings of the National Academy of Sciences of the United States of America 103, 2764–2769 (2006). [PubMed: 16473934]
27. Fonseca VR, Ribeiro F, Graca L, T follicular regulatory (Tfr) cells: Dissecting the complexity of Tfr-cell compartments. Immunological reviews 288, 112–127 (2019). [PubMed: 30874344]
28. Olson MR, Verdan FF, Hufford MM, Dent AL, Kaplan MH, STAT3 Impairs STAT5 Activation in the Development of IL-9-Secreting T Cells. J Immunol 196, 3297–3304 (2016). [PubMed: 26976954]
29. Yang XP, Ghoreschi K, Steward-Tharp SM, Rodriguez-Canales J, Zhu J, Grainger JR, Hirahara K, Sun HW, Wei L, Vahedi G, Kanno Y, O'Shea JJ, Laurence A, Opposing regulation of the locus encoding IL-17 through direct, reciprocal actions of STAT3 and STAT5. Nature immunology 12, 247–254 (2011). [PubMed: 21278738]
30. Wang L, Yu CR, Kim HP, Liao W, Telford WG, Egwuagu CE, Leonard WJ, Key role for IL-21 in experimental autoimmune uveitis. Proceedings of the National Academy of Sciences of the United States of America 108, 9542–9547 (2011). [PubMed: 21593413]
31. Pandiyan P, Zheng L, Ishihara S, Reed J, Lenardo MJ, CD4+CD25+Foxp3+ regulatory T cells induce cytokine deprivation-mediated apoptosis of effector CD4+ T cells. Nature immunology 8, 1353–1362 (2007). [PubMed: 17982458]
32. Pandiyan P, Conti HR, Zheng L, Peterson AC, Mathern DR, Hernandez-Santos N, Edgerton M, Gaffen SL, Lenardo MJ, CD4(+)CD25(+)Foxp3(+) regulatory T cells promote Th17 cells in vitro and enhance host resistance in mouse Candida albicans Th17 cell infection model. Immunity 34, 422–434 (2011). [PubMed: 21435589]
33. Chen Y, Haines CJ, Gutcher I, Hochweller K, Blumenschein WM, McClanahan T, Hammerling G, Li MO, Cua DJ, McGeachy MJ, Foxp3(+) regulatory T cells promote T helper 17 cell development in vivo through regulation of interleukin-2. Immunity 34, 409–421 (2011). [PubMed: 21435588]
34. Botta D, Fuller MJ, Marquez-Lago TT, Bachus H, Bradley JE, Weinmann AS, Zajac AJ, Randall TD, Lund FE, Leon B, Ballesteros-Tato A, Dynamic regulation of T follicular regulatory cell responses by interleukin 2 during influenza infection. Nature immunology 18, 1249–1260 (2017). [PubMed: 28892471]
35. Ray JP, Marshall HD, Laidlaw BJ, Staron MM, Kaech SM, Craft J, Transcription factor STAT3 and type I interferons are corepressive insulators for differentiation of follicular helper and T helper 1 cells. Immunity 40, 367–377 (2014). [PubMed: 24631156]
36. Choi YS, Eto D, Yang JA, Lao C, Crotty S, Cutting edge: STAT1 is required for IL-6-mediated Bcl6 induction for early follicular helper cell differentiation. J Immunol 190, 3049–3053 (2013). [PubMed: 23447690]
37. Wing JB, Kitagawa Y, Locci M, Hume H, Tay C, Morita T, Kidani Y, Matsuda K, Inoue T, Kurosaki T, Crotty S, Coban C, Ohkura N, Sakaguchi S, A distinct subpopulation of CD25(−) T-follicular regulatory cells localizes in the germinal centers. Proceedings of the National Academy of Sciences of the United States of America 114, E6400-E6409 (2017).

38. Ritvo PG, Churlaud G, Quiniou V, Florez L, Brimaud F, Fourcade G, Mariotti-Ferrandiz E, Klatzmann D, Tfr cells lack IL-2Ralpha but express decoy IL-1R2 and IL-1Ra and suppress the IL-1-dependent activation of Tfh cells. Sci Immunol 2, (2017).

39. Malek TR, Castro I, Interleukin-2 receptor signaling: at the interface between tolerance and immunity. Immunity 33, 153–165 (2010). [PubMed: 20732639]

40. Martins GA, Cimmino L, Liao J, Magnusdottir E, Calame K, Blimp-1 directly represses Il2 and the Il2 activator Fos, attenuating T cell proliferation and survival. The Journal of experimental medicine 205, 1959–1965 (2008). [PubMed: 18725523]

41. Gong D, Malek TR, Cytokine-dependent Blimp-1 expression in activated T cells inhibits IL-2 production. Journal of immunology 178, 242–252 (2007).

42. Buenrostro JD, Wu B, Chang HY, Greenleaf WJ, ATAC-seq: A Method for Assaying Chromatin Accessibility Genome-Wide. Curr Protoc Mol Biol 109, 21 29 21–29 (2015).

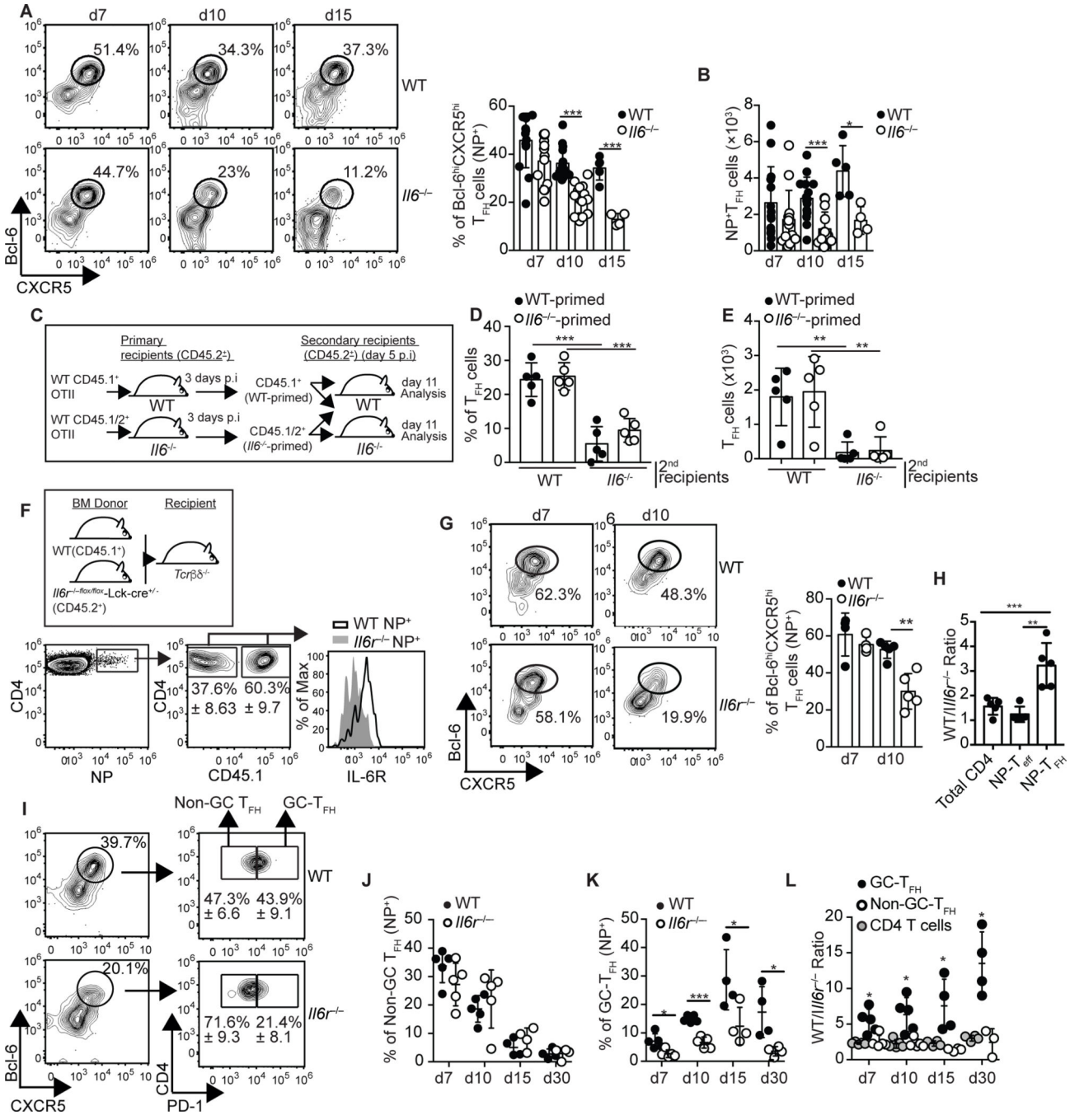

Figure 1. Late IL-6 signaling is required for the accumulation of influenza-specific GC-T_{FH} cells.

(a-b) C57BL/6 (WT) and C57BL/6.*Il6*$^{-/-}$ (*Il6*$^{-/-}$) mice were infected with PR8 and the frequency **(a)** and number **(b)** of NP-specific CD4^{+} T cells with a Bcl-6^{hi}CXCR5^{hi} T_{FH} cell phenotype were evaluated in the mLN at the indicated time points. Representative plots gated on NP-specific CD4^{+} T cells are shown. Data were pooled from three independent experiments from a total of five independent experiments (Data are shown as the mean ± SD, n=4–5 mice per experiment). *P < 0.05, **P < 0.01, ***P < 0.001. P values were determined using a two-tailed Student́s t-test. **(c-e)** Equivalent numbers of CD45.1^{+}CD45.2^{-}

and CD45.1^{+}CD45.2^{+} OTII cells were respectively transferred into CD45.1^{-}CD45.2^{+} WT and CD45.1^{-}CD45.2^{+} *Il6*$^{-/-}$ primary recipient mice. One day later, the recipient mice were infected with PR8-OTII influenza virus. Three days after infection, CD4^{+} T cells from the mLN of WT and *Il6*$^{-/-}$ recipient mice were purified and mixed so that the mixture contained equivalent numbers of CD45.1^{+}CD45.2^{-} (WT-primed) and CD45.1^{+}CD45.2^{+} (*Il6*$^{-/-}$-primed) OTII cells. Cell numbers were then normalized to the concentration of OTII cells and 2×10^{3} cells of the 1:1 mixture of WT-primed and *Il6*$^{-/-}$-primed OTII cells were adoptively transferred into WT and *Il6*$^{-/-}$mice that were previously infected with PR8-OTII influenza 5 days earlier. The frequency **(d)** and number **(e)** of WT-primed and *Il6*$^{-/-}$-primed OTII cells with a PD-1^{hi}CXCR5^{hi} T_{FH} phenotype were determined on day 11 after infection in the mLN. Data are representative of three independent experiments. Data are shown as the mean ± SD (n=5 mice). *P < 0.05, **P < 0.01, ***P < 0.001. P values were determined using a two-tailed Studentś t-test. **(f-l)** *Tcrb*$^{-/-}$ *Tcrd*$^{-/-}$ mice were irradiated and reconstituted with a 50:50 mix of BM from CD45.1^{+} C57BL/6 (WT) and CD45.2^{+} *Il6ra*$^{flox/flox}$-*lck*-$^{cre-/+}$ (*Il6r*$^{-/-}$) donors. Eight weeks later, reconstituted mice were infected with PR8 and cells from the mLN were analyzed at the indicated time points. **(f)** Expression of CD126 (IL-6Ra) in the CD45.1^{+} and CD45.2^{+} NP-specific CD4^{+} T cell compartments. Representative plots on day 7 are shown. **(g)** Frequency of CD45.1^{+} and CD45.2^{+} NP-specific CD4^{+} T cells with a Bcl-6-^{hi}CXCR5^{hi} phenotype. Representative plots are shown. Data in the graph are shown as the mean ± SD (n=5 mice/time point). **(h)** The ratio of WT to *Il6r*$^{-/-}$ CD4^{+} T cells, NP-T_{EFF} (Bcl-6-^{lo}CXCR5^{lo}) and NP-T_{FH} (Bcl-6-^{hi}CXCR5^{hi}) cells on day 10 were calculated (mean ± SD, n=5 mice). **(i)** PD-1 expression within the CD45.1^{+} and CD45.2^{+} NP-specific T_{FH} cell compartments. Representative plots on day 10 are shown. Frequency of GC-T_{FH} (Bcl-6^{hi}CXCR5^{hi}PD-1^{hi}) **(j)** and non-GC-T_{FH} (Bcl-6^{hi}CXCR5^{hi}PD-1^{lo}) **(k)** cells within the CD45.1^{+} and CD45.2^{+} NP-specific CD4^{+} T cell compartments. **(l)** The ratio of WT to *Il6r*$^{-/-}$ NP-specific GC-T_{FH}, NP-specific non-GC-T_{FH}, and total CD4^{+} T cells were calculated (mean ± SD, n=5 mice). Data are representative of three independent experiments. Data are shown as the mean ± SD (n=4–5 mice/time point). *P < 0.05, **P < 0.01, ***P < 0.001. P values were determined using a two-tailed Studentś t-test.

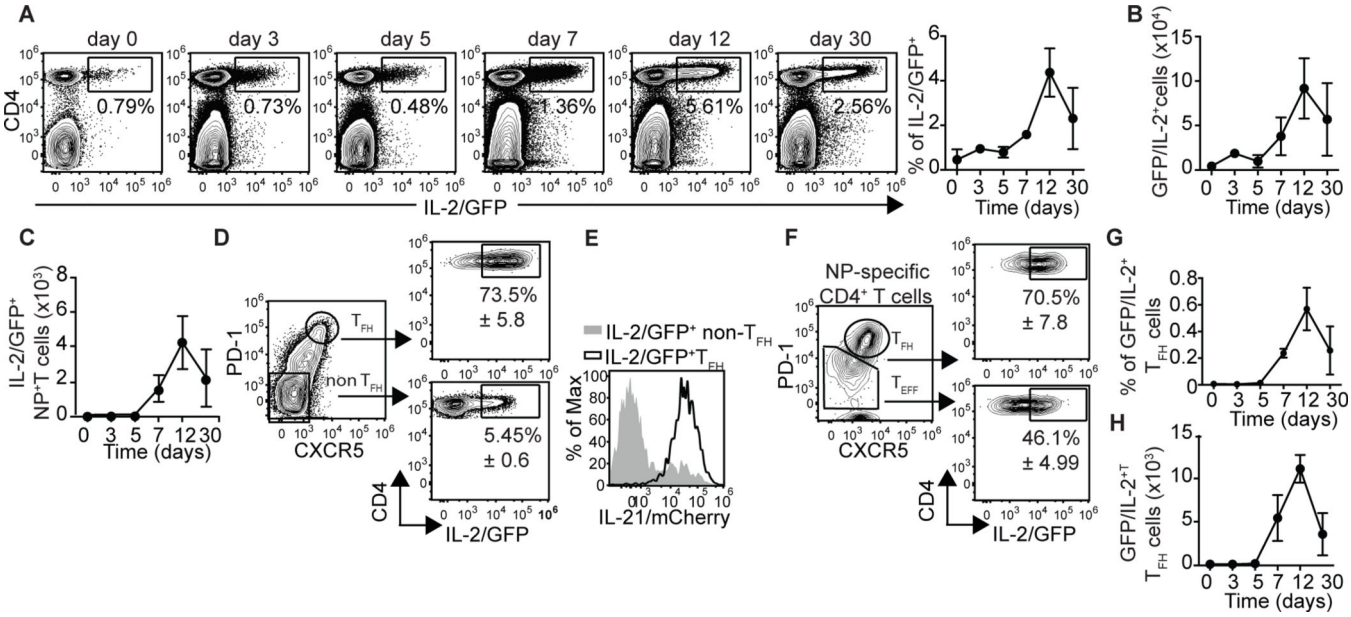

Figure 2. GC-T_{FH} cells produce large amounts of IL-2 at the peak of the infection.

(a-c) *Il21*-mCherry-*Il2*-emGFP reporter mice were infected with PR8 and cells from the mLN were analyzed at the indicated time-points. **(a)** Frequency and **(b)** number of IL2/GFP $^{+}CD4^{+}$ T cells. **(c)** Number of IL2/GFP^{+} NP-specific CD4^{+} T cells. Representative plots are shown. Data in the graphs are shown as the mean ± SD (n=4 mice/time point). Data are representative of three independent experiments. **(d-g)** *Il21*-mCherry-*Il2*-emGFP reporter mice were infected with PR8 and the frequency of IL2/GFP^{+} cells within the PD-1^{hi}CXCR5^{hi} (T_{FH}) and PD-1^{lo}CXCR5^{lo} (non-T_{FH}) CD4^{+} T cell populations were calculated on day 12 after infection. Representative plots gated on CD19-CD4^{+} T cells. (Data are shown as the mean ± SD, n=4 mice/time point). **(e)** Expression of IL-21/mCherry in IL2/GFP^{+} GC-T_{FH} and IL2/GFP^{+} non-T_{FH} cells. Data are representative of three independent experiments **(f)** Frequency of IL2/GFP^{+} cells within the PD-1^{hi}CXCR5^{hi} and PD-1^{lo}CXCR5^{lo} NP-specific CD4^{+} T cell populations on day 12 post-infection. (Data are shown as the mean ± SD, n=4) mice. **(g-h)** Frequency **(g)** and number **(h)** of IL2/GFP^{+} GC-T_{FH} cells at the indicated time points. Data are representative of three independent experiments. Data are shown as the mean ± SD (n=4 mice/time point)

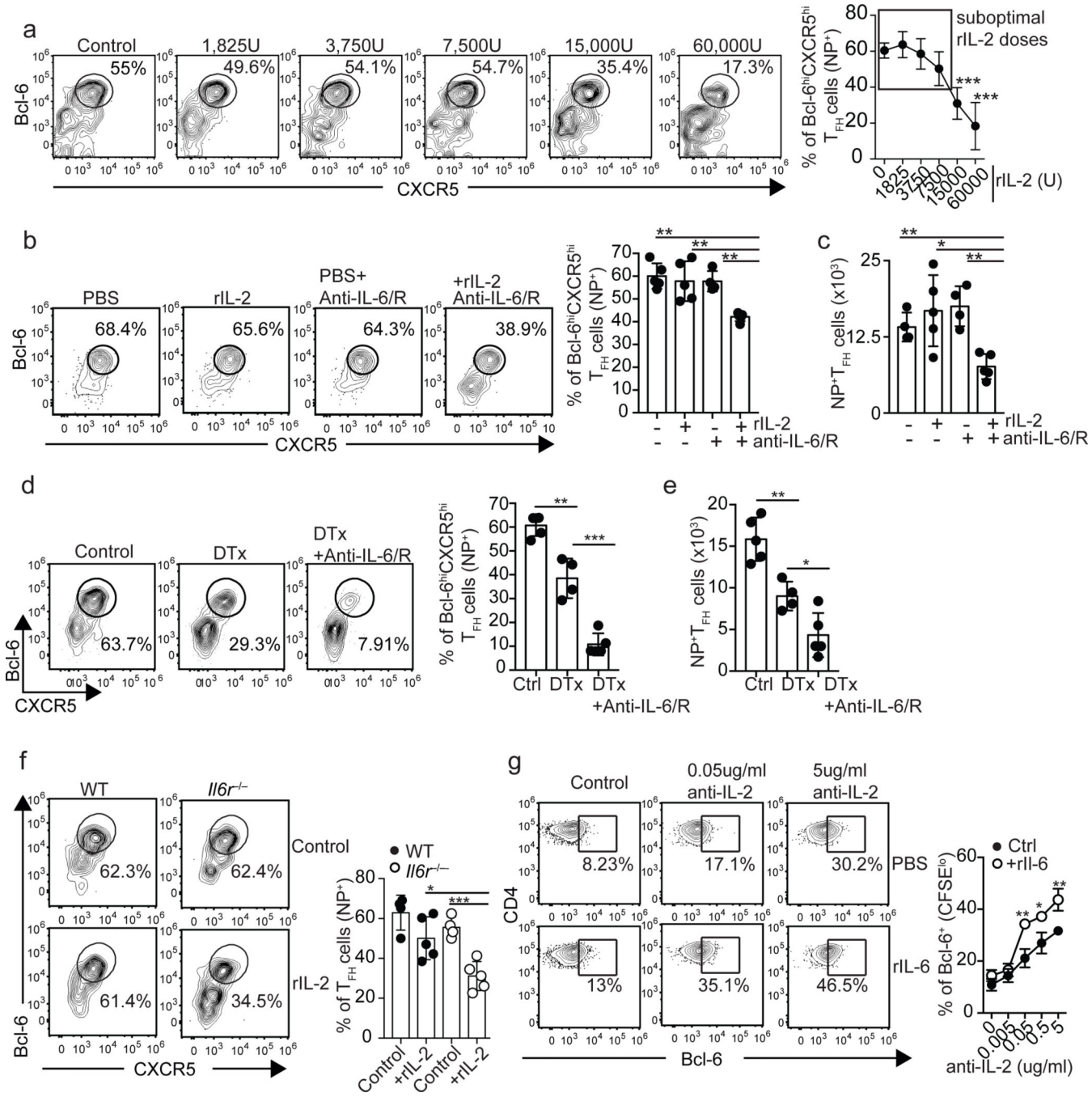

Figure 3. IL-6 signaling is required for sustaining T_{FH} cells developing in a high-IL-2 environment.

(a) B6 mice were infected with PR8 and treated daily with the indicated doses of rIL-2 starting one day after infection. The frequency of NP-specific cells with Bcl-6^{hi}CXCR5^{hi} T_{FH} cell phenotype was determined in the mLN on day 7 after infection. Data in the graph are shown as the mean ± SD (n=4 mice per group). Data are representative of three independent experiments. *P < 0.05, **P < 0.01, ***P < 0.001. P values were determined using a two-tailed Studentś t-test. **(b-c)** B6 mice were infected with PR8, treated daily with

either 7,500U of rIL-2 or PBS alone, or in combination with 250 μg of a mix of anti-IL-6+anti- IL-6/R Abs. The frequency **(b)** and number **(c)** of Bcl-6^{hi}CXCR5^{hi} NP-specific T_{FH} cells were determined in the mLN on day 7 after infection. Representative plots are shown. Data in the graph are shown as the mean ± SD (n=4–5 mice per group). Data are representative of two independent experiments. *P < 0.05, **P < 0.01, ***P < 0.001. P values were determined using a two-tailed Studentś t-test. **(d-e)** Foxp3-DTR–GFP mice were infected with PR8 and treated with either PBS (control) or DT on day 3 after infection. A third group was treated with DT and administered 250 μg of a mix of anti-IL-6+anti-IL-6/R Abs on days 0, 2 and 4 after infection. The frequency **(d)** and number **(e)** of Bcl-6^{hi}CXCR5^{hi} NP-specific T_{FH} cells in the mLN were calculated on day 7 after infection. Representative plots gated on NP-specific CD4$^+$ T cells are shown. Data in the graph are shown as the mean ± SD (n=4–5 mice per group). Data are representative of three independent experiments. *P < 0.05, **P < 0.01, ***P < 0.001. P values were determined using a two-tailed Studentś t-test. **(f)** Irradiated *Tcrb*$^{-/-}$ *Tcrd*$^{-/-}$ mice were reconstituted with a 50:50 mix of BM from CD45.1$^+$ C57BL/6 (WT) and CD45.2$^+$ *Il6ra*$^{flox/flox}$-*lck*-$^{cre-/+}$ (*Il6r*$^{-/-}$) donors. Two months later, chimeric mice were infected with PR8, treated daily with 7,500U of rIL-2 or PBS starting on day 1 after infection, and the frequency of Bcl-6^{hi}CXCR5^{hi} cells within the WT and *Il6r*$^{-/-}$ NP-specific CD4$^+$ T cell compartments calculated on day 7 post-infection in the mLN. Representative plots are shown. Data in the graph are shown as the mean ± SD (n=4–5 mice per group). Data are representative of two independent experiments. *P < 0.05, **P < 0.01, ***P < 0.001. P values were determined using a two-tailed Studentś t-test. **(g)** CFSE-labeled CD4$^+$ T cells from the spleen of naïve B6 mice were activated *in vitro* with plate-bound anti-CD3/CD28 Abs in the presence of the indicated concentration of anti-IL-2 Abs (JES6–1A12+S4B6) and either 10ng/ml of rIL-6 or PBS was added to the cultures. The expression of Bcl-6 in CFSE^{low}CD4$^+$ T cells was assessed at 48h by flow cytometry. Data are representative of four independent experiments. All values were obtained in triplicate and the data are shown as the mean ± SD. *P < 0.05, **P < 0.01, ***P < 0.001P. P values were determined using a two-tailed Studentś t-test.

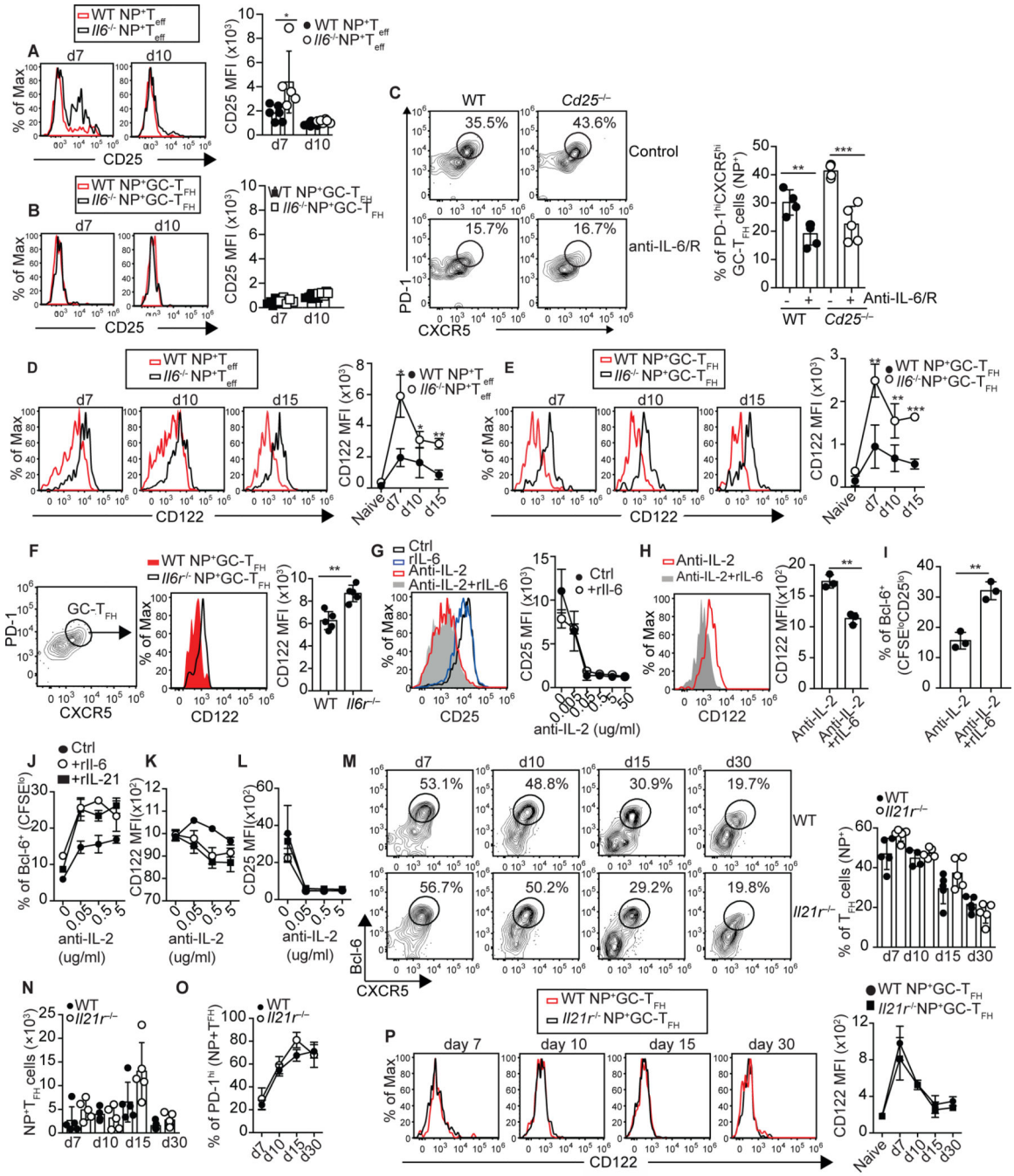

Figure 4. IL-6 signaling limits IL-2 responsiveness by preventing CD122 expression

(a-b) WT and *Il6*$^{-/-}$ mice were infected with PR8 and the expression of CD25 in PD-1^{lo}CXCR5^{lo} NP-specific T_{eff} cells **(a)** and PD-1^{hi}CXCR5^{hi} NP-specific GC-T_{FH} cells **(b)** was examined in the mLN at the indicated time points. Data are representative of three independent experiments. Data in the graph are shown as the mean ± SD (n=5 mice). *P < 0.05, **P < 0.01, ***P < 0.001. P values were determined using a two-tailed Studentś t-test. **(c)** Irradiated *Tcrb*$^{-/-}$*Tcrd*$^{-/-}$ mice were reconstituted with a 50:50 mix of BM from CD45.1^{+} C57BL/6 (WT) and CD45.2^{+} C57BL/6.*Cd25*$^{-/-}$ (*Cd25*$^{-/-}$) donors. Two months

later, chimeric mice were infected with PR8, treated or not with 250 μg of a mix of anti-IL-6 + anti-IL-6/R Abs on days 0, 2, 4, 6 and 8 after infection, and the frequency of PD-1^{hi}CXCR5^{hi} GC-T$_{FH}$ cells within the WT and *Cd25*$^{-/-}$ NP-specific CD4^{+} T cells were examined on day 10 after infection. Representative plots are shown. Data in the graph are shown as the mean ± SD (n=4–5 mice per group). Data are representative of three independent experiments. *P < 0.05, **P < 0.01, ***P < 0.001. P values were determined using a two-tailed Studentś t-test. **(d-e)** Kinetics demonstrating the expression of CD122 in PD-1^{lo}CXCR5^{lo} NP-specific T$_{eff}$ cells **(d)** and PD-1^{hi}CXCR5^{hi} NP-specific GC-T$_{FH}$ cells **(e)** from PR8-infected WT and *Il6*$^{-/-}$ mice. Data are representative of three independent experiments. Data in the graph are shown as the mean ± SD (n=5 mice). *P < 0.05, **P < 0.01, ***P < 0.001. P values were determined using a two-tailed Studentś t-test. **(f)** WT/ *Il6r*$^{-/-}$ mixed BM chimeras were infected with PR8 and expression of CD122 in WT and *Il6r*$^{-/-}$ PD-1^{hi}CXCR5^{hi} NP-specific GC-T$_{FH}$ cells was determined on day 10 after infection. Data are representative of two independent experiments. Data in the graph are shown as the mean ± SD (n=5). *P < 0.05, **P < 0.01, ***P < 0.001. P values were determined using a two-tailed Studentś t-test. **(g-h)** CFSE-labeled CD4^{+} T cells from the spleen of naïve B6 mice were activated *in vitro* with plate-bound anti-CD3/CD28 Abs in the presence of 0.5μg/ml of anti-IL-2 Abs (JES6–1A12+S4B6) and either 10ng/ml of rIL-6 or PBS was added to the cultures. **(g)** Expression of CD25 in CFSE^{lo}CD4^{+} T cells at 48h. **(h)** Expression of CD122 in CFSE^{lo}CD25^{lo} CD4^{+} T cells. **(i)** Expression of Bcl-6 in CFSE^{lo}CD25^{lo} CD4^{+} T cells. Data are representative of three independent experiments. All values were obtained in triplicate and the data are shown as the mean ± SD. *P < 0.05, **P < 0.01, ***P < 0.001P. P values were determined using a two-tailed Studentś t-test. **(j-l)** CFSE-labeled CD4^{+} T were activated *in vitro* in the presence of anti-IL-2 Abs (JES6–1A12+S4B6) and rIL-6 (10ng/ml), rIL-21 (50ng/ml), or PBS was added to the cultures. The expression of Bcl-6 (**j**), CD122 (**k**), and Cd25 **(l)** in CFSE^{low}CD4^{+} T cells was assessed at 48h. Data are representative of two independent experiments. All values were obtained in triplicate and the data are shown as the mean ± SD. **(m-o)** WT and *Il21r*$^{-/-}$ mice were infected with PR8 and cells from the mLN were analyzed at the indicated time points. Frequency **(m)** and number **(n)** of Bcl-6^{hi}CXCR5^{hi} NP-specific T$_{FH}$ cells. **(o)** Frequency of PD-1^{hi} GC-T$_{FH}$ cells within the NP-specific T$_{FH}$ cell population. **(p)** Expression of CD122 in NP-specific GC-T$_{FH}$ cells. Data are representative of two independent experiments. Data in the graph are shown as the mean ± SD (n=5).

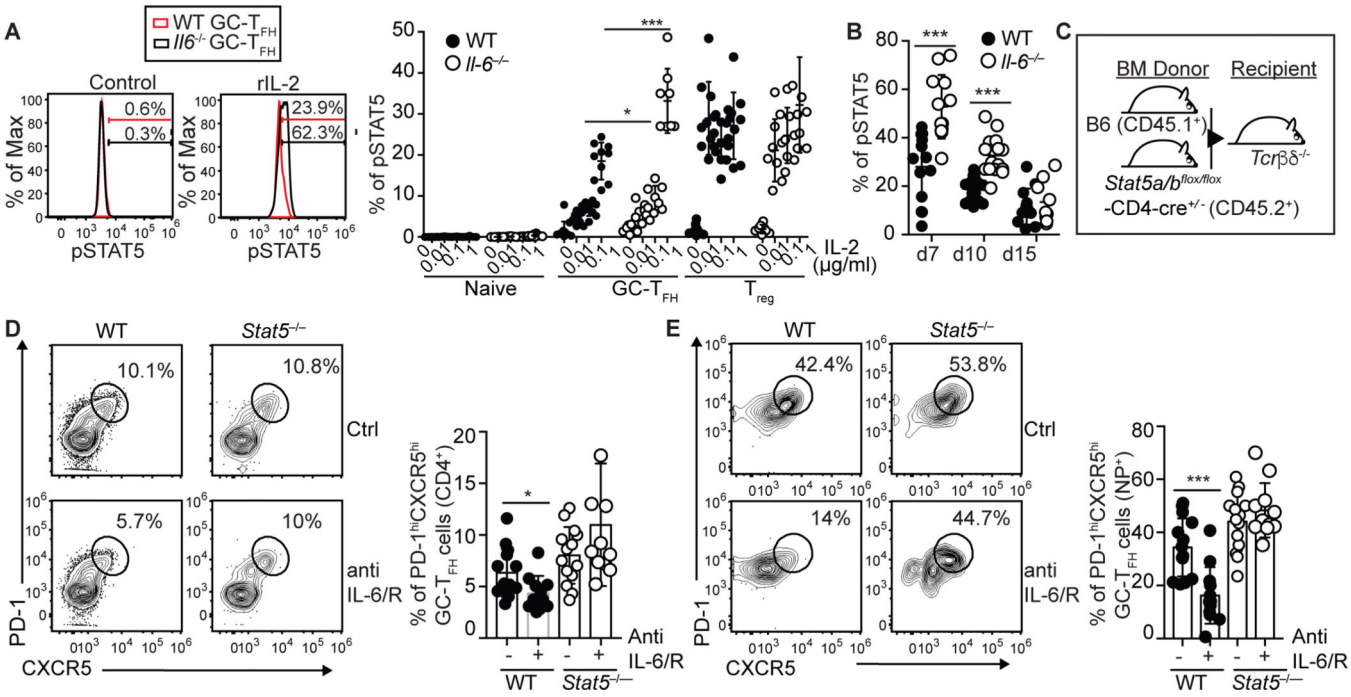

Figure 5. Lack of GC-T$_{FH}$ cells in the absence of IL-6 signaling is STAT5 dependent.

(a) Cells obtained from the mLN of PR8-infected WT and *Il6*$^{-/-}$ mice were stimulated with the indicated amounts of rIL-2 for 15 minutes and STAT5 phosphorylation in PD-1^{hi}Bcl-6^{hi}CXCR5^{hi}CD4$^+$B220$^-$ GC-T$_{FH}$, CD4$^+$B220$^-$Bcl-6^{lo}CXCR5^{lo}CD25$^+$Foxp3$^+$ T$_{reg}$ and in PD-1^{lo}Bcl-6^{lo}CXCR5^{lo}CD4$^+$B220$^-$CD25$^-$Foxp3$^-$ naïve CD4$^+$ T cells was determined by flow cytometry on day 10. Data are representative of three independent experiments. Data are shown as the mean ± SD (n=8–10 mice). **(b)** Kinetic of STAT5 phosphorylation in GC-T$_{FH}$ at different times after infection. Data were pooled from three independent experiments. Data are shown as the mean ± SD. **(c-e)** Irradiated *Tcrb*$^{-/-}$*Tcrd*$^{-/-}$ mice were reconstituted with a 50:50 mix of BM from CD45.1$^+$ C57BL/6 (WT) and CD45.2$^+$ *Stat5a/b*$^{fl/fl}$-*Cd4*$^{cre/+}$ (*Stat5*$^{-/-}$) donors **(c)**. Two months later, chimeric mice were infected with PR8, treated or not with 250 μg of a mix of anti-IL-6 + anti-IL-6/R Abs on days 0, 2, 4, 6 and 8 after infection, and cells from the mLN were analyzed on day 10 post-infection. **(d)** Frequency of PD-1^{hi}CXCR5^{hi} GC-T$_{FH}$ cells within the WT and *Stat5*$^{-/-}$ CD4$^+$ T cell compartments. **(e)** Frequency of PD-1^{hi}CXCR5^{hi} GC-T$_{FH}$ cells within the WT and *Stat5*$^{-/-}$ NP-specific CD4$^+$ T cell compartments. Representative plots are shown. Data in the graph are shown as the mean ± SD. Data were pooled from three independent experiments. *P < 0.05, **P < 0.01, ***P < 0.001. P values were determined using a two-tailed Studentś t-test.

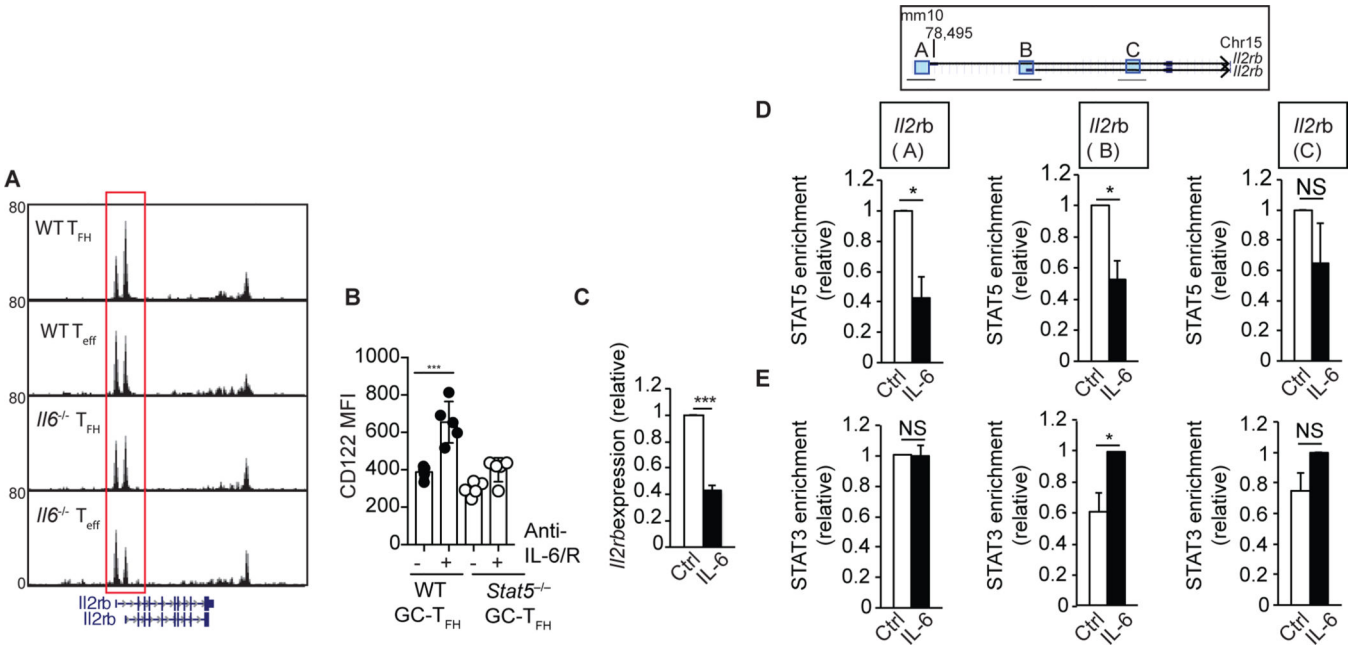

Figure 6. IL-6 signaling limits CD122 expression by inhibiting STAT5 association to the *Il2rb* locus.

(a) OTII (CD45.1$^+$) cells were adoptively transferred into WT and *Il6*$^{-/-}$ recipient mice. One day later, recipient mice were infected with PR8-OTII. Seven days after infection, donor-derived CD45.1$^+$CXCR5^{hi}SLAM^{lo}CD4$^+$CD19$^-$ T_{FH} and CD45.1$^+$CXCR5^{lo}SLAM^{hi}CD4$^+$CD19$^-$ T_{eff} cells were sorted from the mLN of WT and *Il6*$^{-/-}$ recipient mice and ATAC-seq was performed. USCS genome browser tracks displaying chromatin accessibility peaks at the *Il2rb* locus are shown. Results are representative of two biological replicates from two independent experiments. **(b)** WT/*Stat5*$^{-/-}$ mixed BM chimeras were infected with PR8, treated or not with 250 μg of a mix of anti-IL-6+anti-IL-6/R Abs on days 0, 2, 4, 6 and 8 post-infection, and expression of CD122 in WT and *Stat5*$^{-/-}$ PD-1^{hi}CXCR5^{hi} NP-specific GC-T_{FH} cells was determined on day 10 after infection. Data in the graph are shown as the mean ± SD (n=3–5 mice per group). Data are representative of three independent experiments. *P < 0.05, **P < 0.01, ***P < 0.001. P values were determined using a two-tailed Students t-test. **(c-e)** CD4$^+$ T cells from the spleen of naïve B6 mice were activated *in vitro* with plate-bound anti-CD3/CD28 Abs in the presence of rIL-6 or control PBS. **(c)** The expression of *Il2rb* was determined by RT-PCR on day 3. Data are normalized to *Rps18* and represented as fold change in expression relative to the control condition. Data are shown as the mean ± SD (n=5). **(d-e)** CD4$^+$ T cells activated in the presence of IL-6 or control PBS were crosslinked with paraformaldehyde at 72h. Chromatin samples were immunoprecipitated with anti-STAT5 **(d)** or anti-STAT3 **(e)** and the indicated regions of the *Il2r*b locus were monitored by qPCR. Data are shown as the mean ± SEM (n=3). Samples were normalized to the total input followed by subtraction of the isotype control to account for unspecific antibody binding and represented as relative fold change enrichment. Data are shown as the mean ± SEM (n=3). Data are representative of

three independent experiments. *P < 0.05, **P < 0.01, ***P < 0.001. P values were determined using a two-tailed Studentś t-test